

Solid-State Spatial Combiner Modules for TWT Replacement

Robert A. York, Lee-Yin Chen, and Pengcheng Jia

*Department of Electrical and Computer Engineering,
University of California, Santa Barbara, CA 93106
Tel: 805-893-7113, FAX: 805-893-5947, rayork@ece.ucsb.edu*

Abstract:

Significant progress has been made in solid-state spatial power combining under recent DARPA and ARO sponsorship, resulting in multiple demonstrations of power modules that can potentially challenge vacuum electronics in some applications. This paper will focus on a broadband waveguide-based spatial combining approach that shows promise for cost-effective MMIC-based power modules capable of generating hundreds of Watts of CW power at X-band, and scalable to higher frequencies up to Ka-band.

The waveguide-based system uses stacked trays of broadband traveling-wave antenna structures, housed in a metal waveguiding enclosure that is operated in the dominant TE mode. Each antenna is then essentially a waveguide-to-transmission-line transformer that couples energy from the waveguide mode to a set of power amplifier circuits. The antennas can be electrically close for high power density. Thermal management is simplified by virtue of the modular tray architecture and the surrounding metallic walls which provide a convenient heat sink. Power enters and leaves the system in a single well-defined mode and therefore power distribution and collection is simplified. Such arrays also pose a well-defined electromagnetic problem, and consequently significant progress has been made towards optimization of the structures for bandwidth and combining efficiency. The structure affords high combining efficiency, low residual phase-noise, and exhibits desirable graceful degradation characteristics. The use of standard high-volume circuit fabrication processes, a modular design, and off-the-shelf MMICs, coupled with greater reliability, should make these attractive amplifiers for cost-sensitive radar systems.

We will report on recent results in the development of X-band and K-band waveguide-based systems, including 150-Watt level performance using an X-band system in a WR-90 environment. Modeling and optimization techniques will be discussed, as well as other potential enhancements for bandwidth and power-handling. A multi-octave 64-way passive combiner system using oversized coaxial waveguide will also be presented.

Waveguide Combiner Concept

Spatial or quasi-optical power combining arrays have been successfully implemented in a “tray” architecture [1-3], as in fig. 1. The tray approach permits the use of broadband traveling-wave antennas and improved functionality through circuit integration along the direction of propagation. Each tray (fig. 1c) consists of a number of tapered-slotline or finline transitions which coupled energy to and from a rectangular waveguide aperture to a set of MMIC amplifiers. The finline transitions rest over a notched opening in the metal carrier to which the MMIC are attached. When the trays are stacked vertically, as shown in fig. 1b and 1d, the notched carriers form a rectangular waveguide aperture populated with the finline transitions. The use of the waveguide mode to distribute and collect energy to and from the set of amplifiers thus avoids loss mechanisms that would otherwise limit the efficiency in large corporate combiner structures.

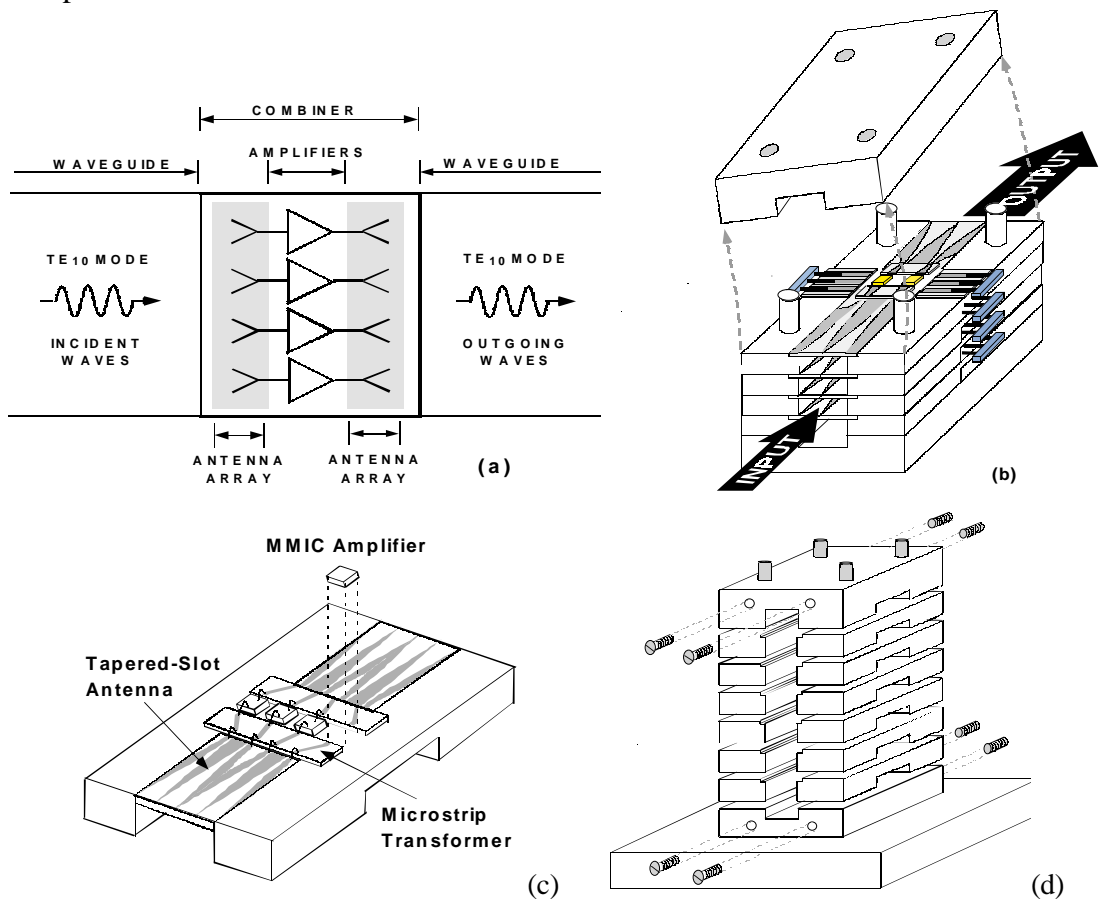


Figure 1— (a) Schematic diagram and (b) graphical illustration of the operating principle of the combiner circuit. (c) individual tray showing finline or tapered-slot transitions and MMICs, along with microstrip interconnects. (d) Assembled system with end-caps, forming input and output waveguide apertures.

Design of the Finline Arrays

The central problem in the design of the finline combiner systems is the electromagnetic design of the tapered-slot or finline transitions. The length and shape of the taper must be chosen to provide the desired impedance level at the MMICs over the desired bandwidth, and thus determines the overall return loss of the structure.

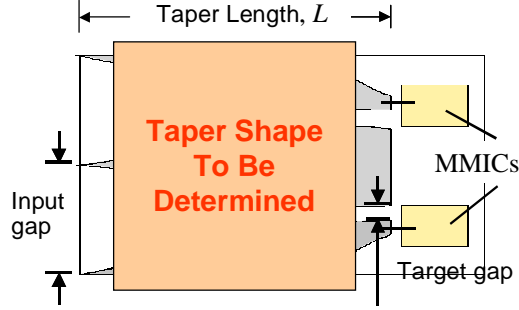


Figure 2: Illustration of the problem statement, to determine the optimum taper shape in a multiple finline structure for matching to a set of MMICs.

The design problem is illustrated in fig.2 and can be summarized as follows: given the physical dimensions of the input and output gaps, along with the waveguide and substrate parameters, find the shape of the taper to realize a specified bandwidth and return loss. The problem is directly analogous to the synthesis of tapered transmission-line impedance transformers. From the theory of small reflections [4] it can be shown that gradual impedance taper on a non-TEM line has an input reflection coefficient

$$\Gamma_{in}(f) = \frac{1}{2} \int_0^{\theta_i} e^{-j\theta} \frac{d}{d\theta} \ln \left(\frac{Z(\theta)}{Z_0} \right) d\theta \quad (1)$$

where z is the position along the taper, L is the taper length, β is the propagation constant, and Z_0 represents the reference impedance at the input end of the taper, and

$$\theta(f, z) = \int_0^z 2\beta(f, z') dz' \quad (2)$$

is the round-trip phase delay to a point z along the taper, as shown in fig.3. The total round-trip phase delay is $\theta_i = \theta(f, L)$.

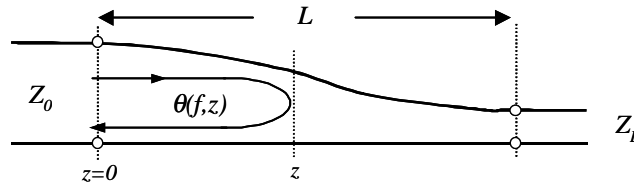


Figure 3: Equivalent tapered transmission-line circuit for modelling the finline array.

The function $Z(\theta)$ describes the variation in impedance along the taper, and is an implicit function of z . In order to maintain an input reflection coefficient $\Gamma < \Gamma_m$ over the desired bandwidth, it has been shown [4,5] that $Z(\theta)$ must take the form

$$\ln \frac{Z(\theta)}{Z_0} = \frac{1}{2} \ln \frac{Z_L}{Z_0} + \Gamma_m A^2 F \left(\frac{2\theta}{\theta_i} - 1, A \right) \quad (3)$$

where Z_L is the terminating impedance, and

$$A = \cosh^{-1}(\Gamma_0 / \Gamma_m), \quad \Gamma_0 = \frac{1}{2} \ln(Z_L / Z_0)$$

$$F(x, A) = -F(-x, A) = \int_0^x \frac{I_1(A\sqrt{1-y^2})}{A\sqrt{1-y^2}} dy$$

and $I_1(x)$ is the modified Bessel function of the first kind and first order. The passband is defined as $\theta_i > 2A$. Assuming the propagation constant is a monotonically increasing function of frequency, the lowest operating frequency is therefore defined by

$$\theta_i(f_0) = 2A \quad (4)$$

which is an implicit relationship between the taper length L , the lower cutoff frequency f_0 , and the maximum reflection coefficient Γ_m .

The main difficulties in applying the above results to the finline arrays are the frequency dependence of the wave impedance and propagation constant, and the difficulty in translating the impedance as a function of θ into a function of z , and subsequently determining the physical parameters required to synthesize the impedance taper. The details for doing this are presented in a recent paper by the authors [11], and the reader is referred to that work for a more complete exposition of the method.

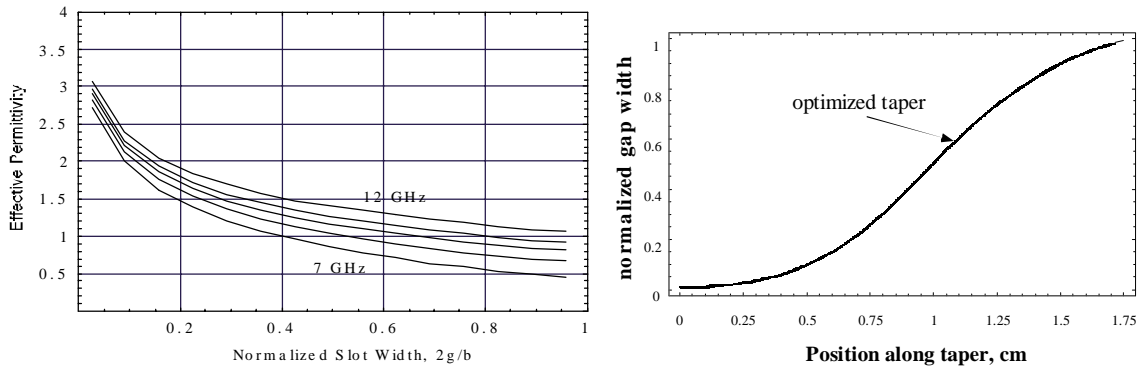


Figure 4: (a) Effective permittivity versus normalized gap width for a 2x2 finline array in WR90 waveguide. (b) Result of optimization procedure for an optimized taper, showing the required normalized gap width vs. location along the structure.

The waveguide aperture and the number of transitions per tray determine the input gap size, but we have not yet addressed the choice of a target gap size. The target gap is determined by the desired impedance level for the MMIC amplifier. For most off-the-shelf MMICs this gap should be chosen for a 50Ω impedance. Unfortunately this is not possible in general for slotline on commonly used substrate materials. Our approach was therefore to choose the smallest realizable gap dimension, giving some impedance that is larger than 50Ω , and include a final impedance transformation to the MMIC in microstrip as part of the slot-line-to-microstrip transition.

Once the problem has been defined, the propagation constant (or effective permittivity) in the finline array is determined, and the optimum taper computed from (3). Figure 4a summarizes the results of the propagation constant analysis for a 2-tray (4 antenna) system. Using these results, an “optimized” taper was computed for an input reflection coefficient of -20dB , shown in fig. 4b. The taper design was tested experimentally by terminating the slots in a resistive matched load, using 100Ω chip resistors as depicted in fig. 5a. Two trays were then stacked and placed centrally in a WR90 waveguide, and return loss measurements were made. The measured return loss is shown in fig. 5b, along with the theoretical predictions using the theory of sections III-IV. Excellent agreement is observed over the measured bandwidth, which was limited to 8.2-12.4 GHz due to the calibration standards used. Discrepancies between the two curves are attributed to some additional series inductance from the bonding of the chip resistors.

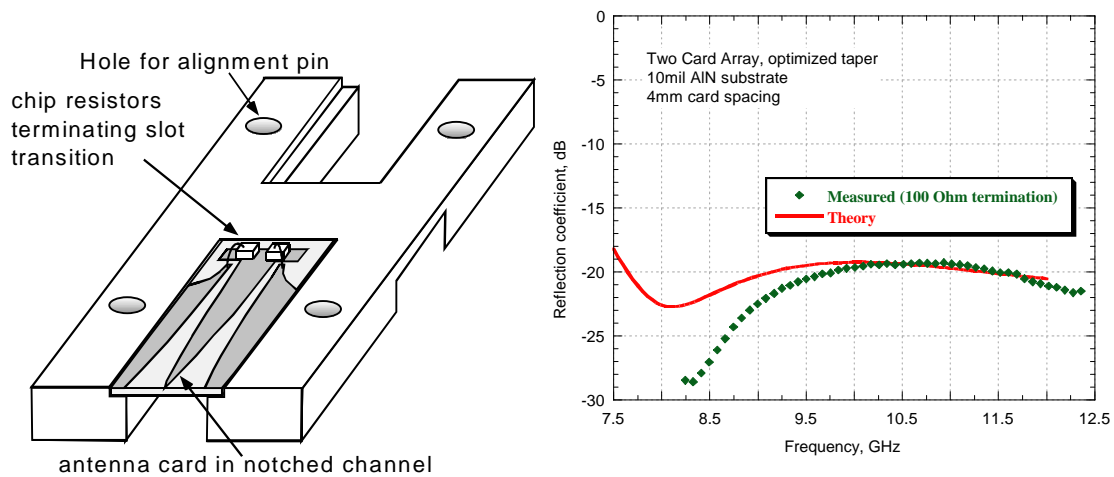


Figure 5: (a) Finline transitions terminated in resistive loads for design verification. (b) Comparison of measured reflection coefficient with theoretical predictions for a 2x2 finline array in WR90 waveguide, using the taper design of fig. 6.

MMIC Amplifiers

The MMIC amplifiers used in this work were commercially available parts from Texas Instruments (Now TriQuint-TI), TGA9083-EEU. The amplifiers were mounted on individual Cu-Mo carriers. External bias capacitors were epoxy-mounted in close proximity to the MMIC amplifiers for low-frequency stabilization. Careful attention was paid in construction to minimize bondwire lengths and avoid potential electrical shorting of components due to excessive epoxy.

The nominal specifications for this MMIC amplifier was 6-8 Watts CW at 7-9 Volt drain bias over the range 6.5-11 GHz, with a small signal gain of 19dB and power-added efficiency (PAE) of 33-40 %. On-chip active gate biasing was used to simplify the biasing setup. Each MMIC amplifier was characterized in isolation for performance screening and bias setup. Fig. 6 shows a plot of output RF power vs. frequency (linear scale) for the MMICs used in this work. Fig. 7 illustrates the output power vs. input power measurements at 9 GHz, showing some differences in saturated power and linear gain among MMIC amplifiers. On average, the actual maximum output RF power from a single MMIC was about 6.8 Watts when driven into saturation at 9 V bias.

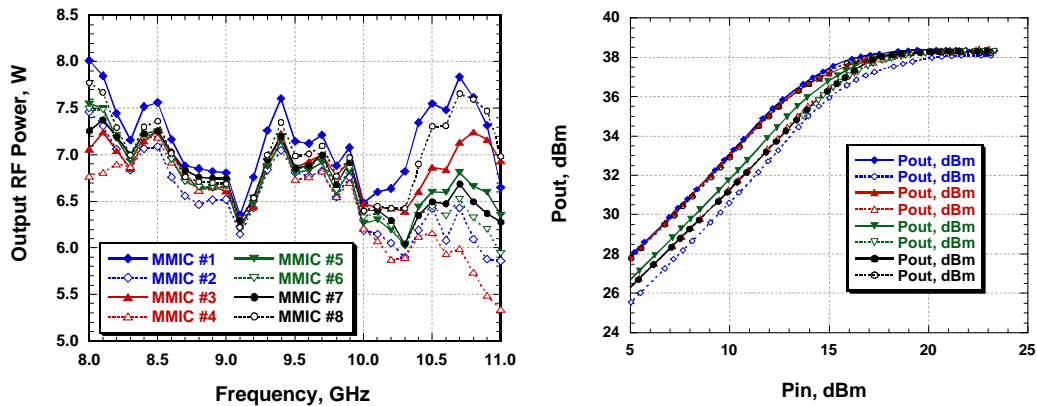


Figure 6: (a) Power measurements for individual MMIC amplifiers versus frequency for 21 dBm input power. (b) Pout vs. Pin measurements for individual MMIC amplifiers.

X-band Results

40W 8-MMIC (4x2) Array

Initial efforts focused on a 4-tray system with 2 MMICs per tray. An assembled 4x2 array in an aluminum package is shown in figure 7a. Coaxial-to-waveguide adapters were used to create a coaxial-based environment for measurements. A TWT (Traveling Wave Tube) amplifier was used during testing to provide sufficient input drive to saturate the amplifier. CW Measurements were taken up to 11 GHz, where the performance of MMIC amplifiers starts to degrade. This data is shown in figure 7b.

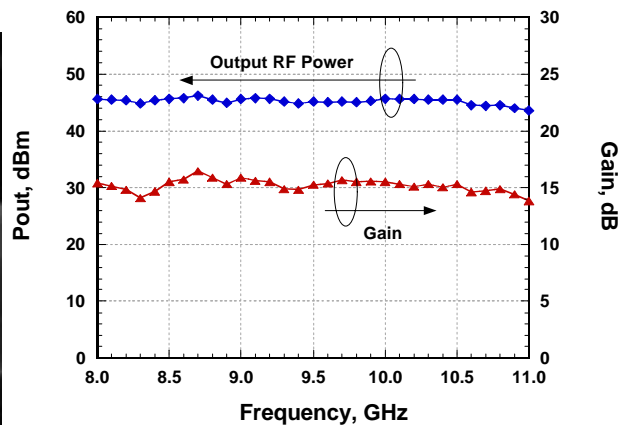
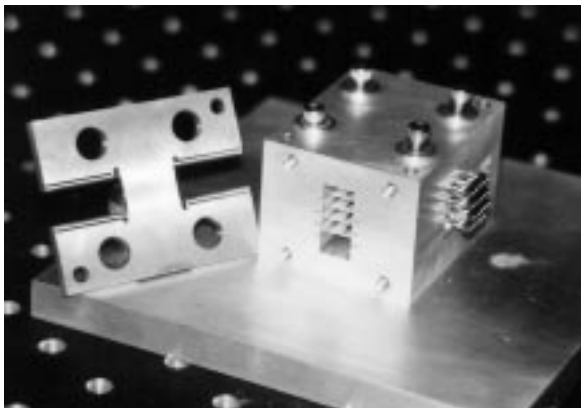


Figure 7: (a) Photograph of the combiner circuit based on 2x4 arrays. (b) Power measurements for the combiner circuit. Pin = 30 dBm.

A maximum output power of about 41 Watts was observed at 8.7 GHz, with a corresponding gain of about 16.5 dB. The gain varies within the range from 13.8 to 16.5 dB, indicating a remarkably broadband characteristic, with only less than ± 1.4 dB gain variation. The PAE of the combiner circuit fluctuates, in the range from 17 to 27 %, as the frequency varies. About 150 Watts of DC power and 17 Amperes of drain current by average were consumed by the eight MMIC amplifiers when the combiner was in operation. Thermocouples were used and

attached to various positions on the body of test fixture for temperature measurement. About 41 °C of temperature difference existed between the bottom surface of metal carrier right underneath the MMIC amplifiers and the base plate, which was about 25 °C. These numbers suggest that the MMIC amplifiers were operated under a benign condition and the waste heat has been removed efficiently during the measurements. Additional details for this combiner are summarized in [3].

120W 24-MMIC (6x4) Array

A second generation design using 6 trays with 4 MMICs per tray was then built. The circuit layout on a single tray is shown in Fig. 8. Each MMIC amplifier, which was pre-mounted on to a Cu-Mo heat-spreader, was attached directly onto the test fixture using conducting silver epoxy and cured subsequently at 175°C. The trays themselves were machined from copper and gold-plated to facilitate mounting and soldering of components. A microstrip taper was used as a broadband impedance transformer between the tapered-slot antenna and MMIC amplifier.

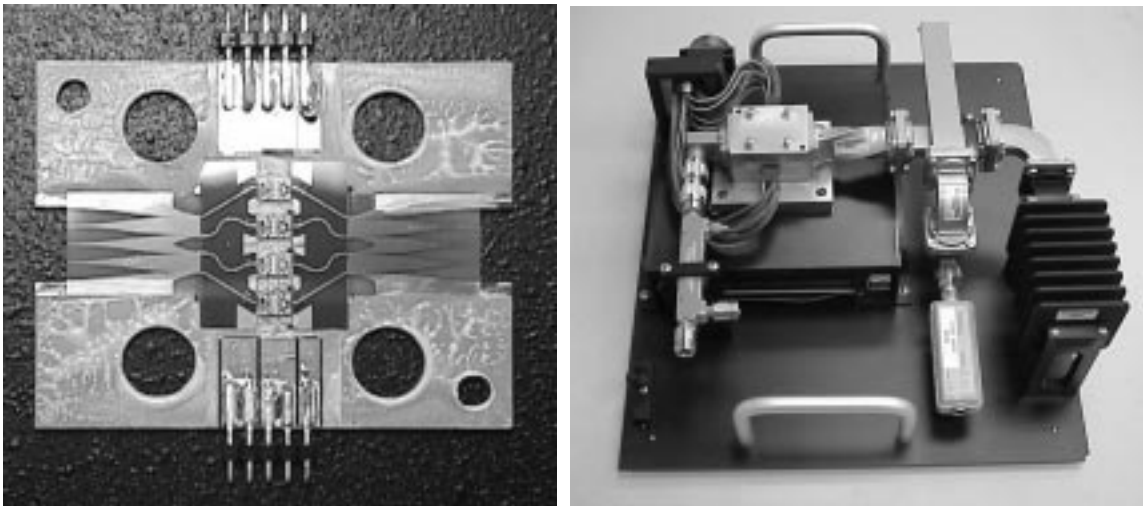


Figure 8: (a) Photograph of the combiner circuit based on 2x4 arrays. (b) Power measurements for the combiner circuit. Pin = 30 dBm.

An overview of the complete rack-mounted combiner system, along with an empty tray in front of the combiner, is shown in Fig. 8b. A heat sink equipped with fins and a horizontal-flow cylindrical fan was used as a baseplate to enhance the heat-dissipating capacity. To reduce the thermal resistance between the MMIC amplifiers and heat sink, non-conductive thermal grease was applied between adjacent trays and top/bottom covers. However, the thermal grease resulted in extra electrical resistance between the groundings of adjacent trays. Individual grounding was provided to each tray to avoid possible oscillation problem. All bias leads were connected to a common power hub as shown.

The MMIC amplifiers were operated under CW condition with frequency sweep from 8.4-11GHz. The total of twenty-four MMIC amplifiers, which were biased at 8 Volts of drain voltage, consumed about 43 Amperes of drain current and 246 Watts of DC power on average. The dissipated DC power presented a significant swing in value between 300 and

400 Watts during the frequency sweep. The PAE of the combiner circuit fluctuated between 13 and 34 % as frequency varied, in correlation with the DC power dissipation. The output power and gain versus frequency data is shown in figure 9a. The gain flatness is somewhat degraded as compared with the 4-tray system of fig. 7, which is a result of using a finline taper that was optimized for a 2-tray system. With refinements to the antenna shape, similar gain flatness would be anticipated. Nevertheless, the combiner system demonstrated excellent performance generating up to 120W CW.

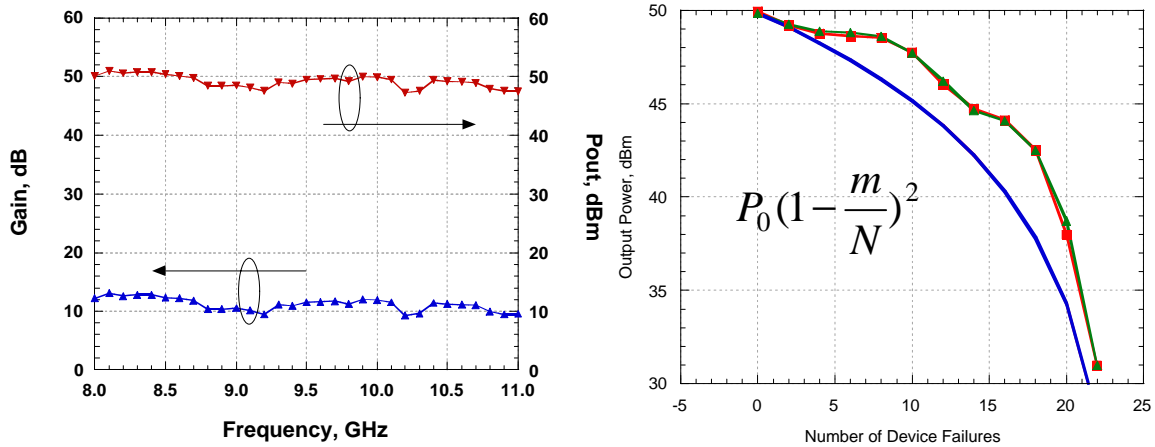


Figure 9: (a) Measured output power (CW) and gain versus frequency for the 6x4 system. (b) Graceful degradation characteristics.

The graceful degradation characteristics are summarized in fig. 9b, and compared against a simple power-conservation expression. The combiner circuit lost about 57 % of original output power when half of the devices were turned off. Ideally it should be 50 % if the devices were ideally isolated. No catastrophic failure was observed as a result of the loss of these amplifiers. Additional details on this system can be found in [10].

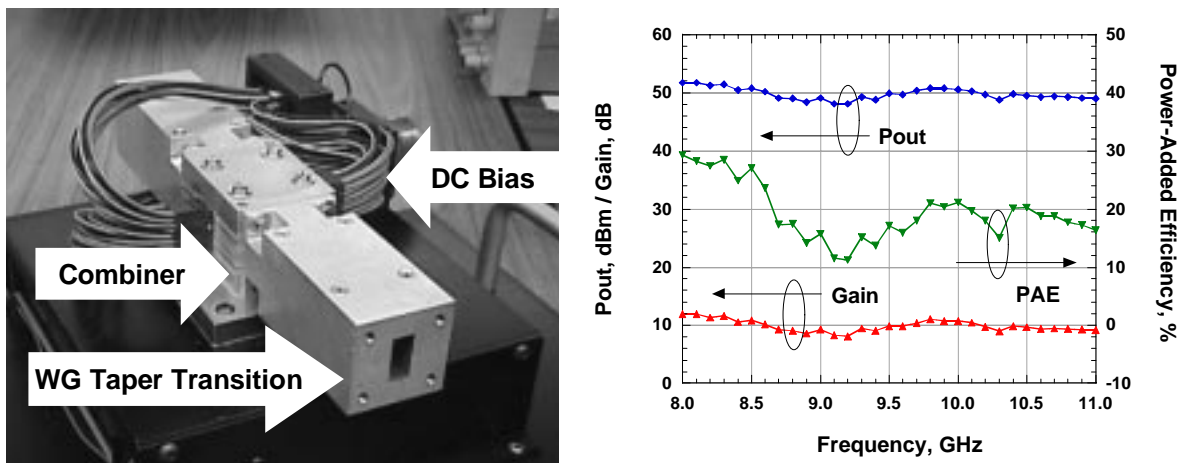


Figure 10 – (a) Overview of the combiner circuit based on an 8x4 array, including two linear waveguide taper sections mounted at the input/output ports, providing standard waveguide (WR-90) apertures. (b) Power performance for the 8x4 combiner system, with $P_{in} = 40$ dBm and MMICs biased at 8 Volts.

150W 32-MMIC(8x4) Array

To demonstrate the additional capacity and modularity of the combiner design, an 8-tray, 32-MMIC system was constructed, based on the same tray design as in fig. 8. In this case, the additional trays enlarged the waveguide aperture beyond the standard WR-90 dimensions, requiring the use of a tapered-feed structure as shown in fig. 10. Otherwise the operation conditions were similar. The measured data is summarized in figure 10b. Excellent performance was observed with up to 150W being generated by the combiner system. Increased gain variation as compared with the 4-tray and 6-tray systems was again attributed to the non-optimized antenna structure.

K-band Combiner Efforts

Under ARO sponsorship, UCSB is currently attempting to improve the design and modelling of the waveguide combiners, building on the demonstrations at X-band summarized above. This includes extending the concept to mm-wave frequencies, which requires the use of oversized waveguiding enclosures in order to accommodate a sufficiently large number of devices and trays. A K-band (20GHz) prototype is under development and is shown in figure 11a. Measurements on the passive structure with a 6x4 array of terminated finline antennas is shown in fig. 11b, suggested good low-loss and broadband characteristics in the desired operating band. This initial design is a linearly scaled version of the X-band passive system reported above.

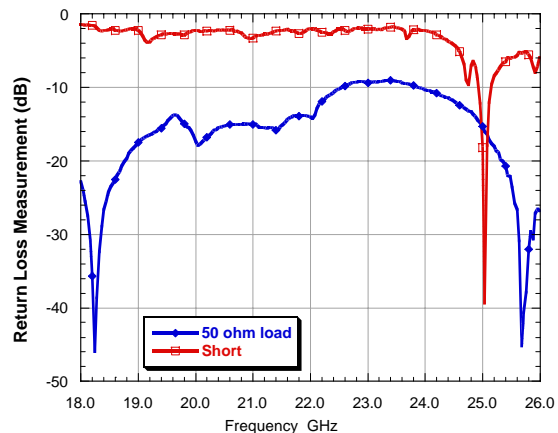
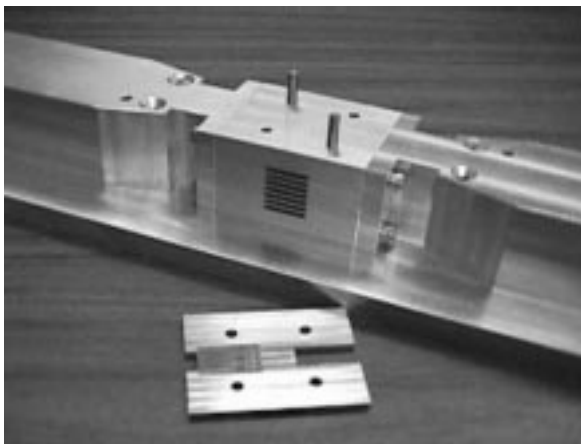


Figure 11 – (a) Photo of 6-tray K-band (18-20GHz) combiner prototype. (b) Measured data on the passive structure with terminated finline arrays.

UCSB is currently developing a hybrid flip-chip amplifier technology for K-band amplifiers using commercial off-the-shelf (COTS) discrete devices for use in these combiner systems. In this technology a COTS device is flip-chip bonded to an AlN carrier using thermal-compression bonding to a set of raised gold “bumps” patterned into the appropriate device footprint. The AlN substrate carries all additional circuitry including cpw transmission-line, thin-film resistors and capacitors, etc. A simple one-stage amplifier design is shown in fig. 12a (inset) along with measured small signal data. A tray design based on this amplifier

design is shown in fig. 12b, with 4 amplifiers per tray. UCSB is currently assembling this system and will report on the results in a future publication.

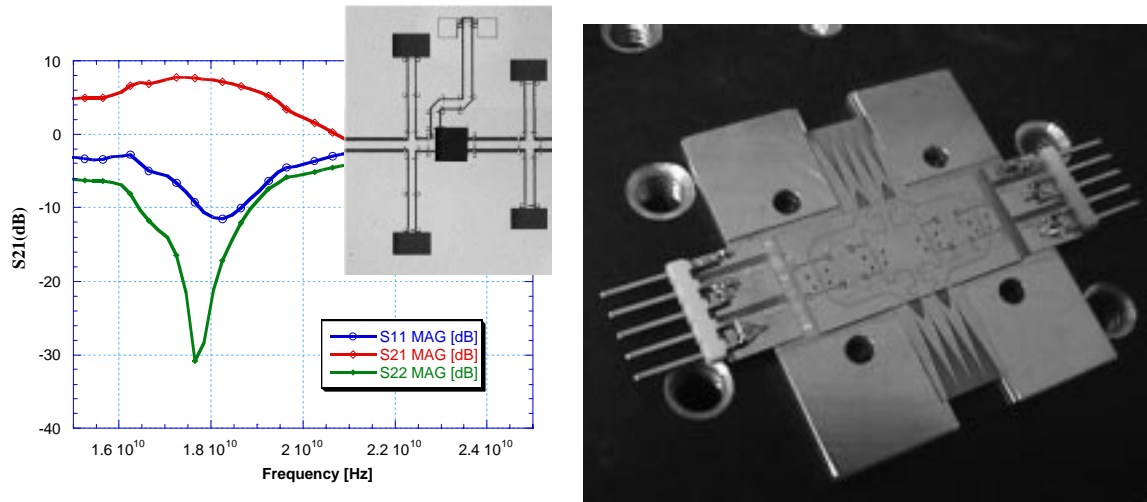


Figure 12 – (a) Measured small-signal performance of an K-band amplifier using flip-chip mounted commercial pHEMT on an AIN carrier. (b) Single tray for K-band system using 4 amplifiers per tray.

Coaxial Combiner Structure

UCSB is also investigating topologies which can be used to greatly increase the bandwidth and number of devices. One attractive possibility is shown in fig. 13, which is a coaxial waveguide-based combiner system. The use of a TEM-mode combiner means that there is no cutoff frequency for the structure, providing a much wider operating band. In addition, the perfect rotational symmetry of the structure greatly simplifies the modeling, since the array analysis can be reduced to the analysis of a single unit cell with appropriate floquet boundary conditions.

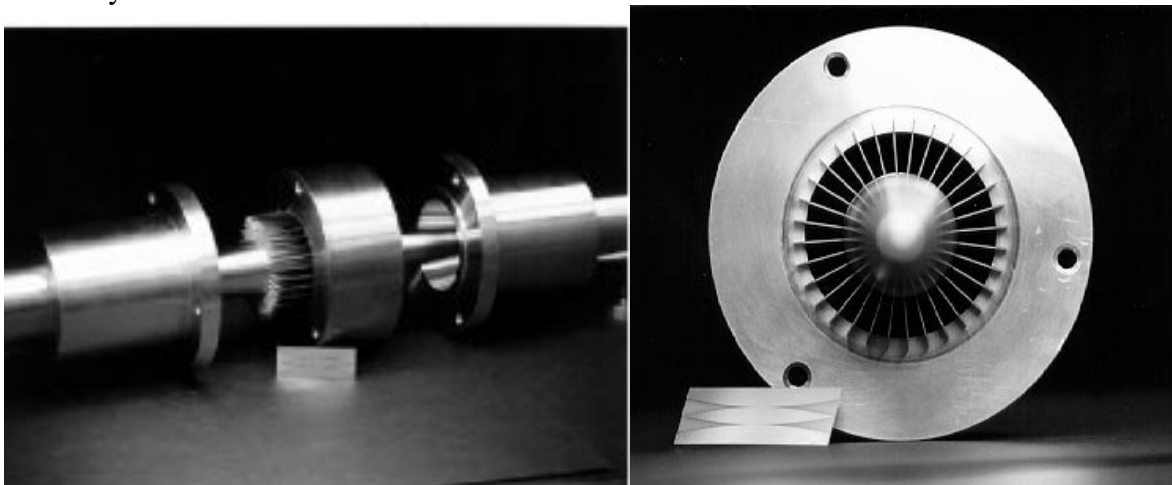


Figure 13 – (a) Exploded view of coaxial combiner. (b) Axial view of center section with finline cards.

Initial theoretical and experimental efforts on the prototype of fig. 13 are summarized in fig. 14, showing insertion loss and return loss for a 32-card (64-way) combiner. The system is capable of operation from 4-20GHz with excellent broadband matching and low loss, and the measured results compare favorably with modeling efforts. Currently UCSB is attempting to implement an active version of this combiner using a combination of GaAs pre-amplifiers and GaN-based power-amplifiers.

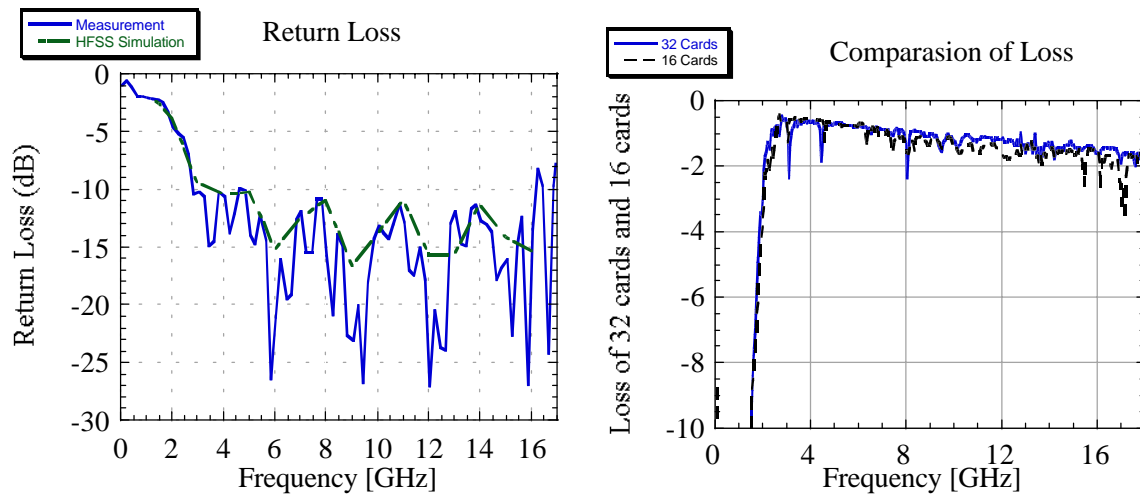


Figure 14 – (a) Return loss and (b) insertion loss for the coaxial combiner.

Conclusions

Exciting progress has been made in the development of high-power solid-state amplifiers using a spatial combining approach within an enclosed waveguide structure. The combiners presented herein have demonstrated high output power and combining efficient with broadband performance. The combiners exhibit graceful degradation, and the modular design provides for convenient fabrication and manufacture. The excellent heat-sinking capacity of the combiner has been verified during power measurements, with as much as 415 Watts of DC power dissipated by the MMIC amplifiers in one design. The approach provides a broadband impedance match to the MMICS and is transparent to the device technology. The results so far have been encouraging, suggesting a promising outlook for our combining system to compete with the currently dominating traveling-wave tube amplifiers (TWTAs) in high-power applications.

Acknowledgements

This work was funded under the DARPA MAFET program through a subcontract from the HRL Laboratories in Malibu, CA (contract N66001-96-C-8625), and by an ARO MURI program (grant DAAG55-98-1-0001) through a subcontract from Caltech.

References

1. N.-S. Cheng, "Waveguide-Based Spatial Power Combiners", Ph.D. Dissertation (ECE Technical Report #99-08), Dept. of Electrical and Computer Engineering, University of California, Santa Barbara CA, 93106, June 1999.
2. A. Alexanian and R.A. York, "Broadband Spatially Combined Amplifier Array using Tapered Slot Transitions in Waveguide", *IEEE Microwave Guided Wave Lett.*, vol. 7, no. 2, pp. 42-44, Feb 1997
3. N.-S. Cheng, A. Alexanian, M. G. Case, D. B. Rensch and R. A. York, "40 Watt CW Broadband Spatial Power Combiner Using Dense Finline Arrays", *IEEE Transactions on Microwave Theory and Techniques*, vol. 47, no. 7, July 1999.
4. D. M. Pozar, *Microwave Engineering*, 2nd Ed., New York, NY: John Wiley & Sons, 1998.
5. R.W. Klopfenstein, "A Transmission-Line Taper of Improved Design," *Proc. IRE*, vol. 442, pp. 31-35, January 1956.
6. Schieblich, J.K. Piotrowski, J.H. Hinken, "Synthesis of Optimum Finline Tapers using Dispersion Formulas for Arbitrary Slot Widths and Locations", *IEEE Trans. Microwave Theory Tech.*, vol. MTT-32, pp. 1638-1644, Dec 1984.
7. C.Verver and W. Hoefer, "Quarter-wave matching of waveguide-to-finline transitions", *IEEE Trans. Microwave Theory Tech.*, vol. MTT-32, pp. 1645-1648, Dec. 1984.
8. L.P. Schmidt and T. Itoh, "Spectral Domain Analysis of Dominant and Higher Order Modes in Fin-lines", *IEEE Trans. Microwave Theory Tech.*, vol. MTT-28, pp. 981-985, Sept 1980
9. T. Itoh, "Spectral Domain Immitance Approach for Dispersion Characteristics of Generalized Printed Transmission Lines", *IEEE Trans. Microwave Theory Tech.*, vol. MTT-28, pp. 733-737, July 1980.
10. N.-S. Cheng, P. Jia, D. B. Rensch and R. A. York, "A 120-Watt X-Band Spatially Combined Solid-State Amplifier", *IEEE Trans. Microwave Theory Tech.*, Dec 1999.
11. P. Jia, L-Y Chen, N-S. Cheng, and R.A. York, "Design of Waveguide Finline arrays for Spatial Power Combining", submitted to *IEEE Trans. Microwave Theory Tech.*, Feb 2000.
12. Pengcheng Jia, *et al.*, "Analysis of a Passive Spatial Combiner Using Tapered Slotline Array In Oversized Coaxial Waveguide", to appear at the *IEEE MTT-S International Microwave Symposium 2000*